CHAPTER VI

FIELD INVESTIGATION USING FULL-SCALE TESTS

6.1 General

Although the study of the axle loads identification using the small-scale tests, as explained in chapter V, can provide useful information toward the real application. Due to the complexity of the dynamic vehicle-bridge interaction, the study might not be able to guarantee the actual identification performance of the methods when they are applied to the real bridges. Therefore, the investigation using full-scale models of bridge and vehicles is necessary. In this chapter, the study of the axle loads identification is further investigated using the full-scale tests.

6.2 Description of the Tested Bridge

In the followings, the real bridge in the west outer-ring roads at KM28+170.31 crossing Bang-Noi canal was chosen as the tested bridge and used to install the instrumentation system as shown in Figure 6.1. This bridge is chosen because its ease to accessibility for instrumentation and experiments, its properties such as span length of bridge and traffic density are good representative for the most bridge, and the bridge deck slab type is the most popular type of the constructed bridges in Thailand.

The bridge is a 25-span simply supported structure carrying three traffic lanes (one direction). The total length of the bridge is nearly 250 m. with each span length of about 10.0 m. below the bridge is a canal. Therefore, in order to easily access, the approach span is chosen to install sensors. This span bridge is a prestressed concrete bridge with 10 m span length and 14 m width as shown in Figure 6.2. The precast plank slabs with thickness 0.50 m (include concrete topping) are simply supported bridge which are placed on the reinforced concrete cross beam with cross section 0.50x0.70 m which is supported by concrete piers with cross section 0.35x0.35 m. The concrete of the bridge structure has an elastic modulus of 26 GPa and a weight of 24.5 kN/m^2.
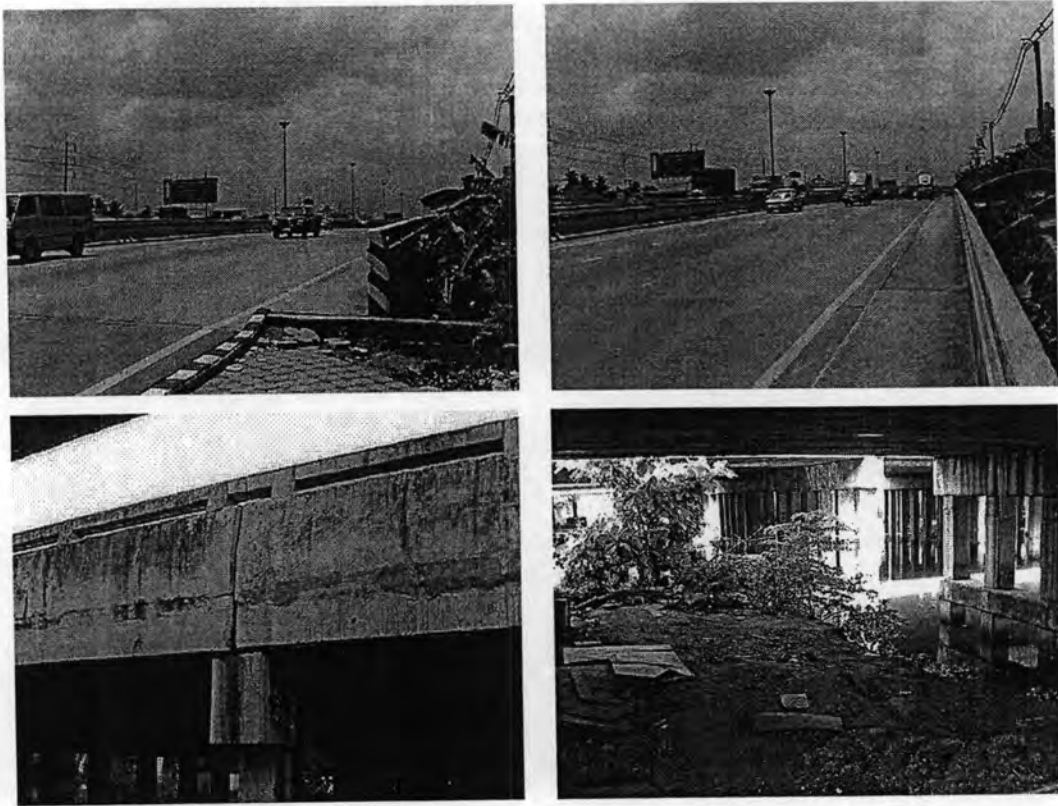
Figure 6.1 Photographs of tested bridge in the west outer-ring roads at KM28+170.31 crossing Bang-Noi canal
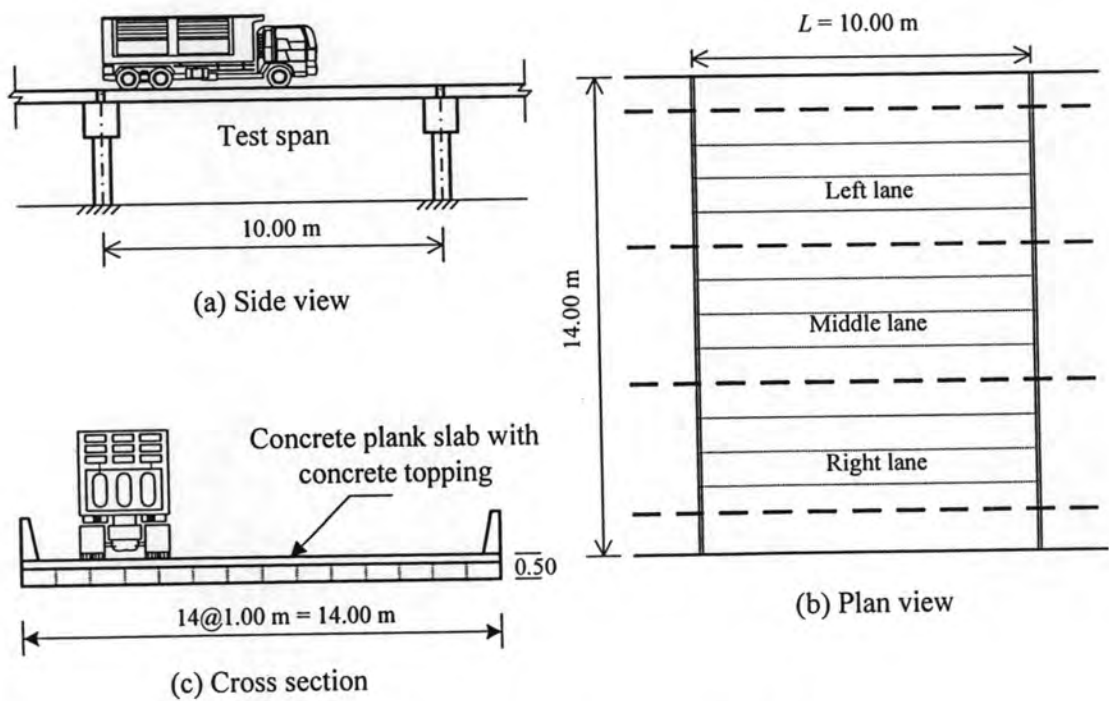

Figure 6.2 Configuration of tested bridge

6.3 Full-Scale Test Setup

The control room under the tested span is constructed to setup the instrumentation system as shown in Figure 6.3. In this room, the instrumentations consisted of strain gauges, signal cables, data logger, computer and the others are installed as shown in Figure 6.4. The bending moments of the bridge induced by moving vehicles are measured at three sections, i.e. at $L/3$, $L/2$ and $2L/3$. To do so, twelve strain gauges are attached beneath the bridge deck for each section and their readings are used to compute the bending moment as in Eq. (5.1). Two laser axle detectors are installed at the entrance and exit positions of the test span in order to measure the position and speed of the vehicle. In addition, a CCTV camera is installed on the post beside the bridge for video recording. The total of thirty-six strain gauges at three bridge sections, two axle detector sensors, and CCTV camera are all connected to the same data acquisition unit and are simultaneously recorded as shown in Figure 6.5. The sampling frequency of the data of 1024 Hz is used for all tests and the moving averaging technique with re-sampling of 256 Hz is employed. Figure 6.6 shows photographs of the instruments used in full-scale tests. The diagram of instrumentation system is shown in Figure 6.7.
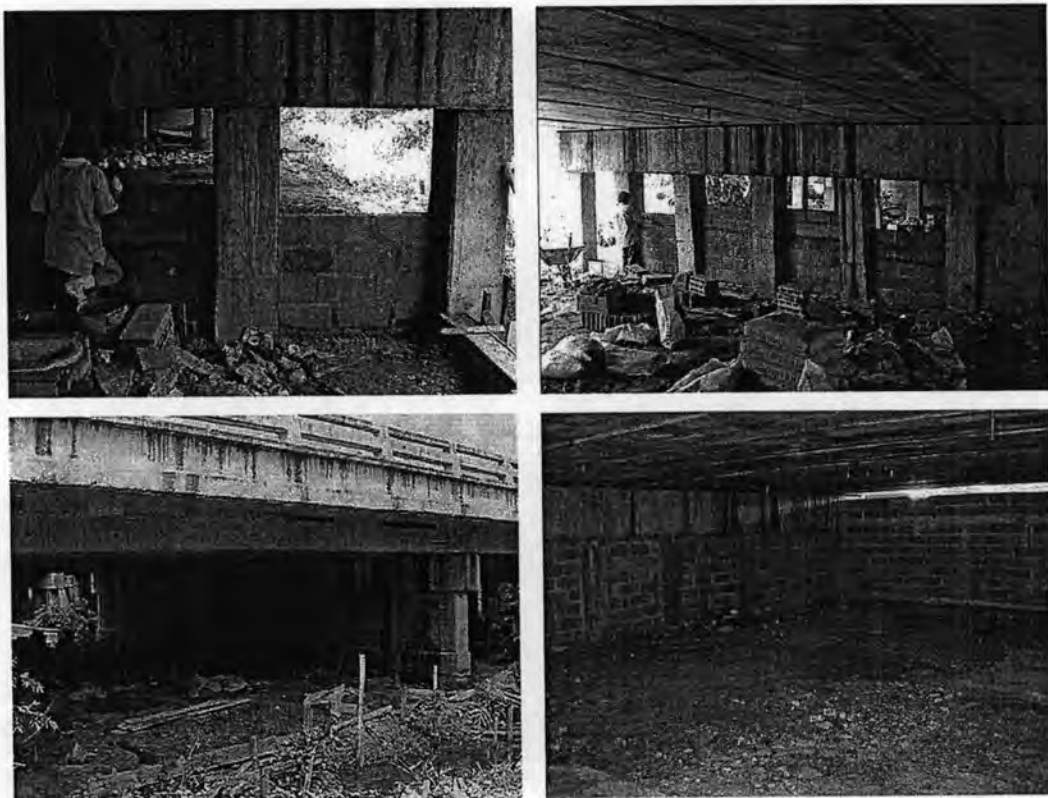

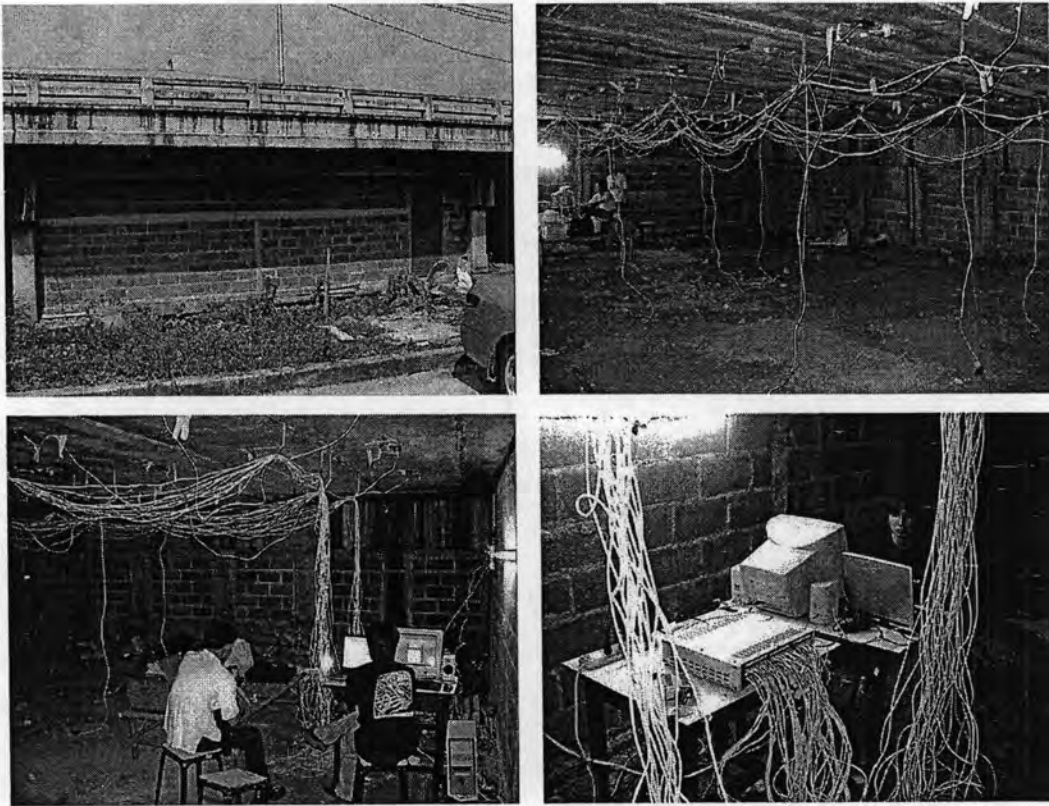Figure 6.3 Construction of control room under the bridge

Figure 6.4 Photographs of the instrument system in control room
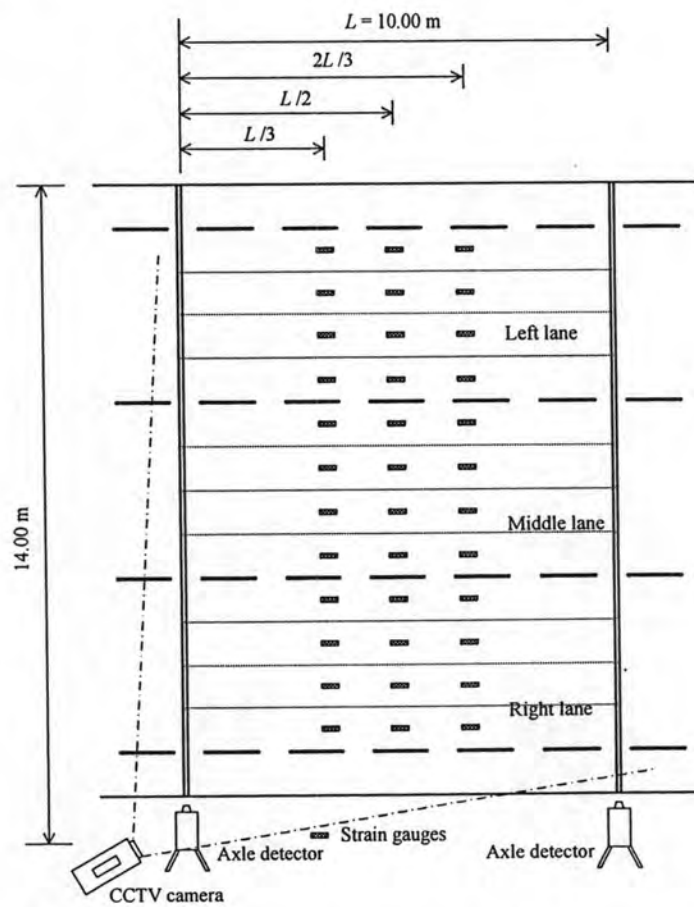
Figure 6.5 Strain gauges, Axle detector and CCTV camera locations
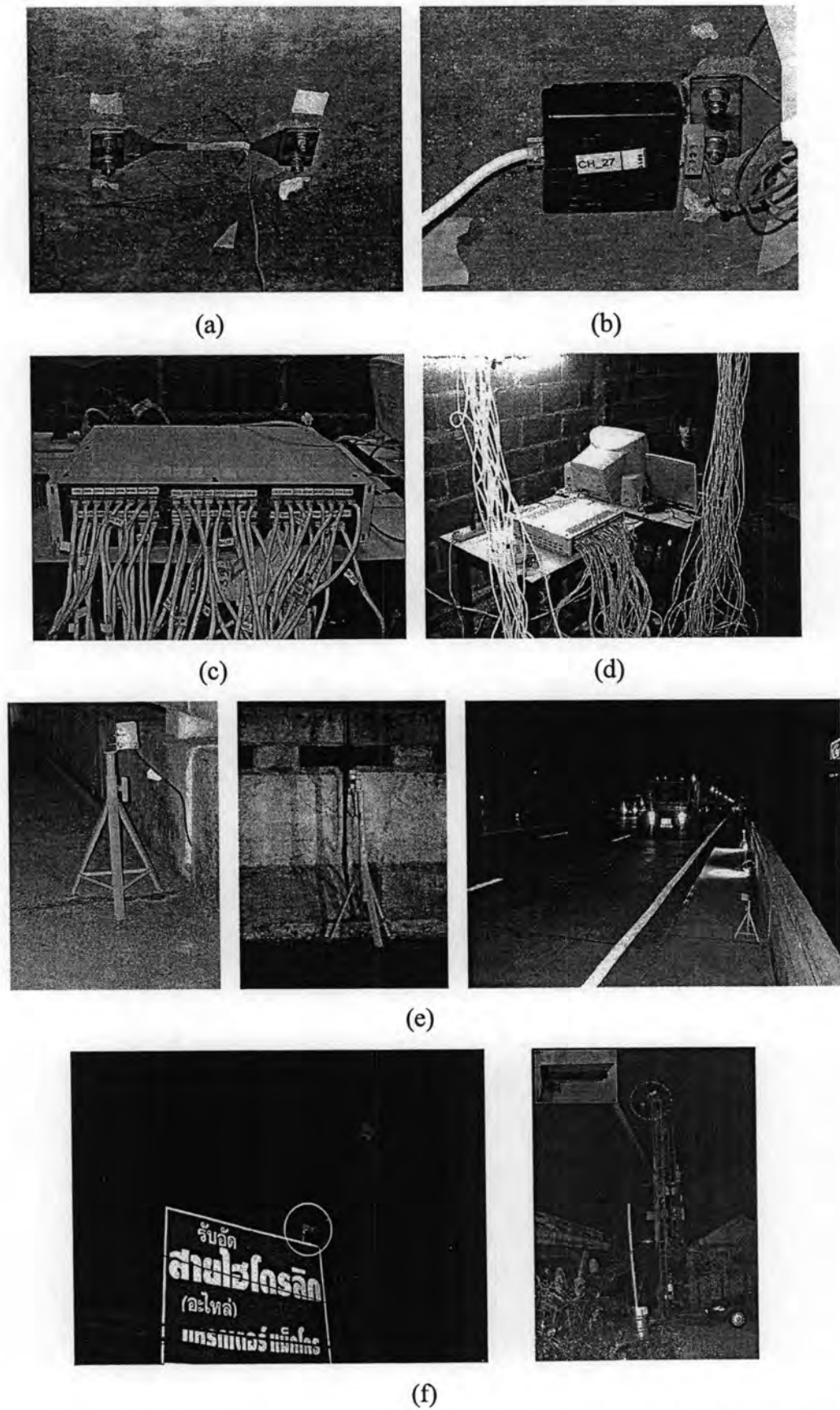
(a)

(b)

(c)

(d)

(e)

(f)

Figure 6.6 Photographs of instruments used in full-scale test: (a) strain gauge, (b) completion bridge box, (c) 48-channel data logger, (d) computer, (e) axle detector and (f) CCTV camera
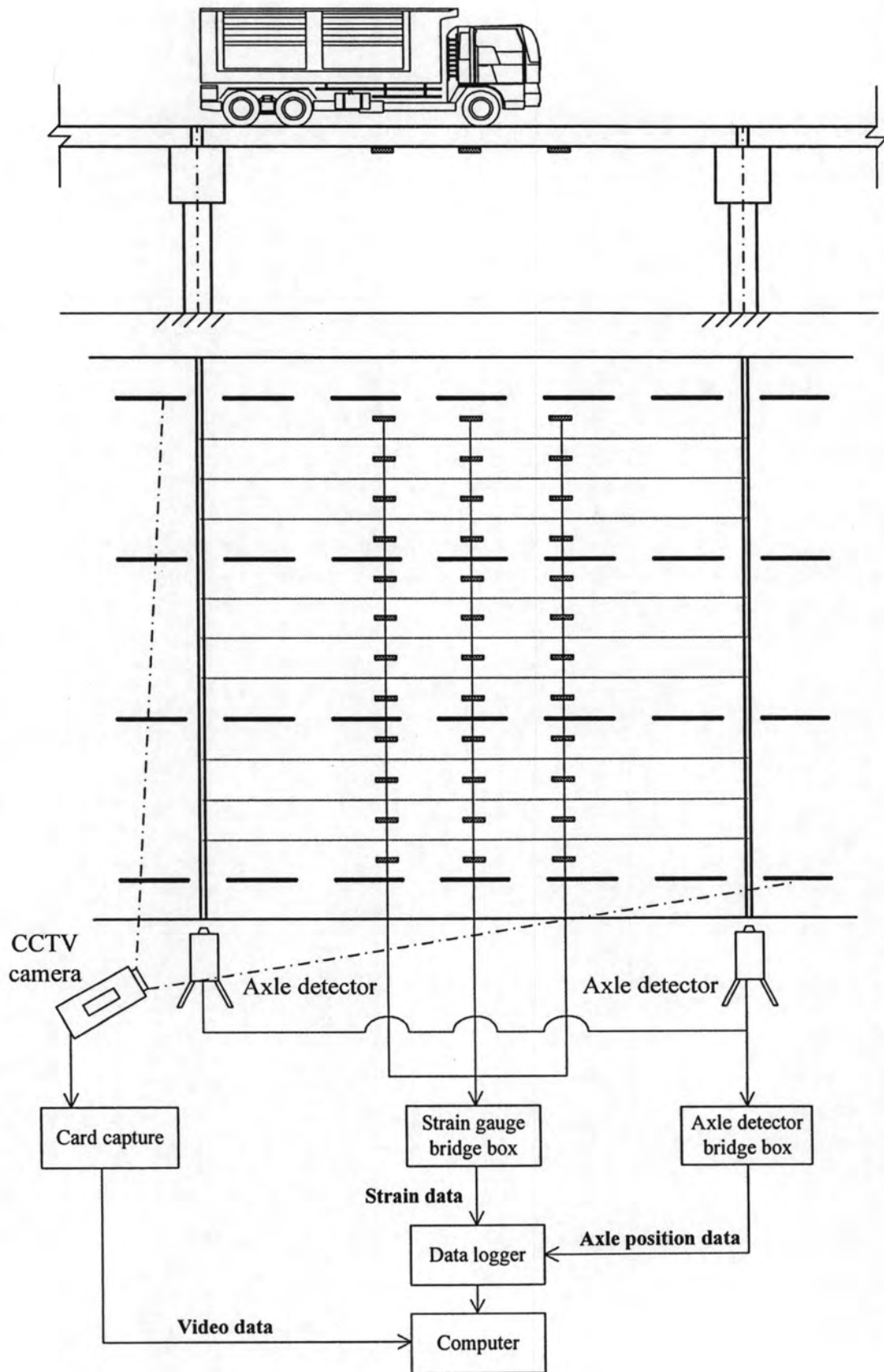
Figure 6.7 Diagram chart of the data acquisition system

6.4 Full-Scale Test Configuration

The full-scale tests are conducted by the passages of a truck with known axle weights with various speeds and different traffic lanes. The truck used in these tests is a standard 10-wheel truck in Thailand as shown in Figure 6.8. The truck having gross weight case of 200, 230 or 260 kN as listed in Table 6.1 is driven across the bridge with different speeds and travelling paths. Since the control of truck speed is rather difficult, three levels of speeds ranging from 5 to 12 m/s (18-45 km/hr) are considered and are denoted as slow (5-8 m/s), moderate (8-10 m/s) and fast (10-12 m/s) speed levels. For each speed level, the tests are conducted for three repetitive runs to guarantee the correctness of the measured results. Due to the difficulty on conducting the test in the right traffic lane, only the travelling paths in the left and middle traffic lanes are investigated. Based on the obtained bending moments of the bridge at three sections, the axle weights of the truck are identified employing the Method I and Method II as mentioned in Chapter 3. Since the second and third axles are very close and are difficult to accurately identified (Yu, 2004 and Asnachinda, 2008). They are modeled by a single rear axle acting through their center.
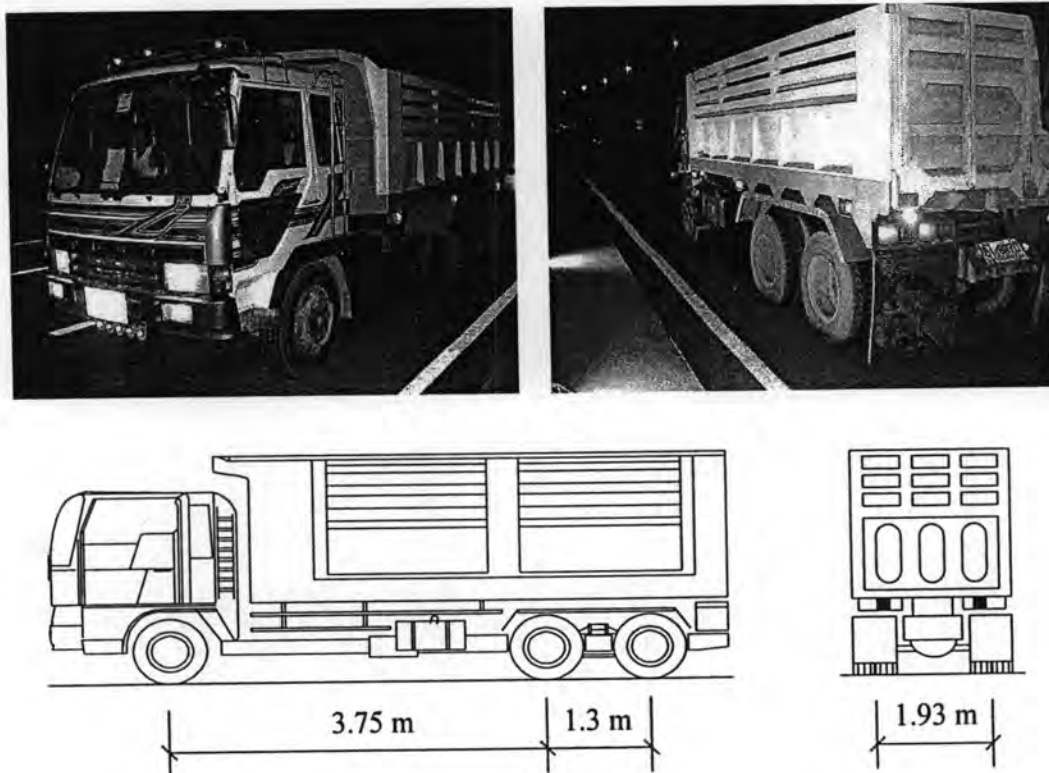

Figure 6.8   Configuration of 10-wheel tested trucks

Table 6.1 Configuration of truck weight case

No.	Truck weight case	Front axle wt. (kN)	Middle & rear axle wt. (kN)	Gross truck wt. (kN)
1	200 kN	45.18	79.67	204.53
2	230 kN	43.46	92.76	228.98
3	260 kN	55.32	98.69	252.69

The calibration test of bridge by a truck with known weight and axle spacing moving at very slow speed is adopted. Since there might be some incorrectness in the physical properties due to materials and instruments, the calibration test is necessary in order to obtain the most accurate identified solution. The calibration test is the procedure employed to determine the proper parameters of the material (i.e. flexural stiffness, *EI*, which is a multiplication of elastic modulus and moment of inertia) and to correct the signal measurement recorded by instruments. The flexural stiffness of bridge is determined based on testing in static or least dynamic condition by measuring the bending moments induced by recognized axle loads vehicle moving at crawl speed. The measured bending moment is corrected with constant coefficient as follow:

$$Z_{calibrated} = \alpha Z_{measured} \tag{6.1}$$

where $Z_{calibrated}$ is the calibrated bending moment matrix

$Z_{measured}$ is the measured bending moment matrix

α is the correction coefficient used in flexural stiffness correction

Based on an optimization, the coefficient matrix can be determined by minimizing the residual error between the analytical and measured bending moments. A relevant least squares objective function is expressed as

$$\Delta(\alpha, k_c) = \sum_{j=1}^{k} \left[\sum_{i=1}^{NN} \left(Z_{analytical}^i - \alpha Z_{measured}^i \right)^2 \right]_j \tag{6.2}$$

where $Z_{analytical}$ is the analytical bending moment matrix with the size of $k \times NN$ (measured section and number of data) constructed from theoretical bridge model. The analytical bending moment is calculated with estimated bridge stiffness from construction drawing. It is noted that the sectional bending moments used in identification are adopted from average value of bending moments converted from strain readings installed at the same section. The objective function in Eq. (6.2) is

optimized using computer program, MATLAB with "fminunc" command utilizing Quasi-Newton algorithm. By assuming flexural stiffness of each section to be the same, the optimized flexural stiffness coefficients are obtained for each travelling path, left, middle and right as listed in Table 6.2.

Table 6.2 Calibrated coefficients of the full-scale bridge model

Travelling paths (Lane)	Flexural stiffness coefficients
Left	$\alpha = 2.0710$
Middle	$\alpha = 2.3070$
Right	$\alpha = 2.9818$

6.5 Strains and Bending Moments of the Bridge

Figures 6.9(a) and 6.9(b) plot the typical measured signals from the twelve strains at the $L/2$ section for the case of the 230 kN truck moving at moderate speed of 29 km/hr on the bridge in left and middle lanes, respectively. Based on those strains, the strain distributions across the bridge section, when the distance of front axle of the truck is about 8.2 m, are extracted and plotted in Figure 6.10. Similar to the small-scale investigation, the effect of bridge torsion on the strain readings is firstly investigated. Since the width to span length ratio of the bridge is quite large, it is clearly seen from the figures that the bridge torsion seriously affects the obtained strain values. However, it is found that this torsion effect can be substantially eliminated if the bending moments of the bridge are considered as shown in Figures 6.11(a) to 6.11(c). These results encourage the use of a 2-D bridge model with the bridge moments input instead of the use of a complex 3-D bridge model. Thus, in the followings, the Method I and Method II are employed to identify the axle loads of the vehicle from bridge bending moments adopting 2-D bridge model. Moreover, these figures demonstrate that the continuity effect from the side spans on bending moment of the bridge is perfectly zero. Therefore, the bridge can be considered as a simply supported beam.

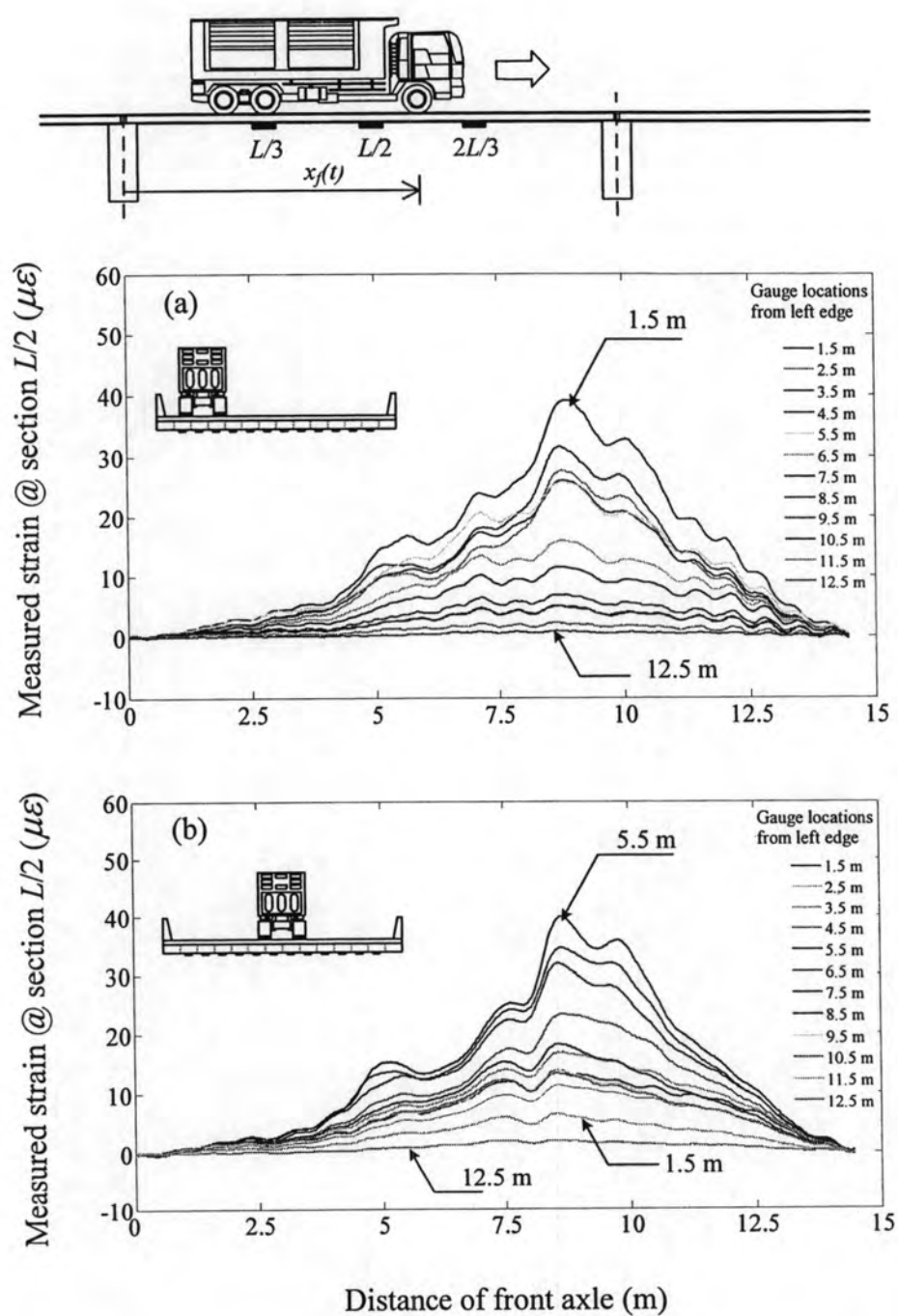Figure 6.9 Typical measured strains at section $L/2$ under various travelling paths of a truck: (a) left lane and (b) middle lane
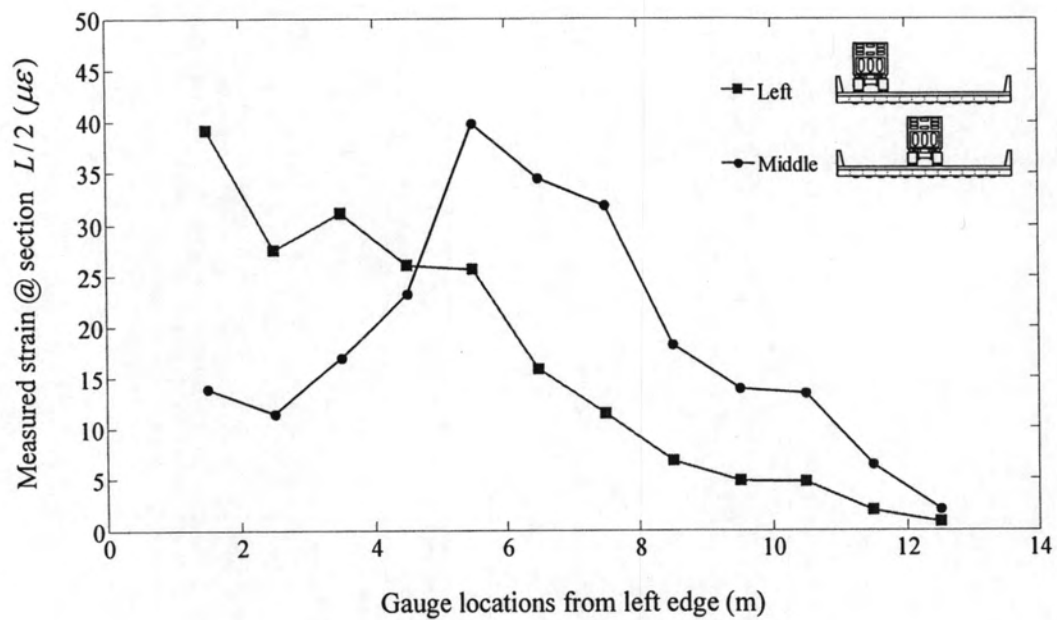
Figure 6.10 Typical measured strain distributions across section $L/2$ under a passage of truck on left and middle lanes
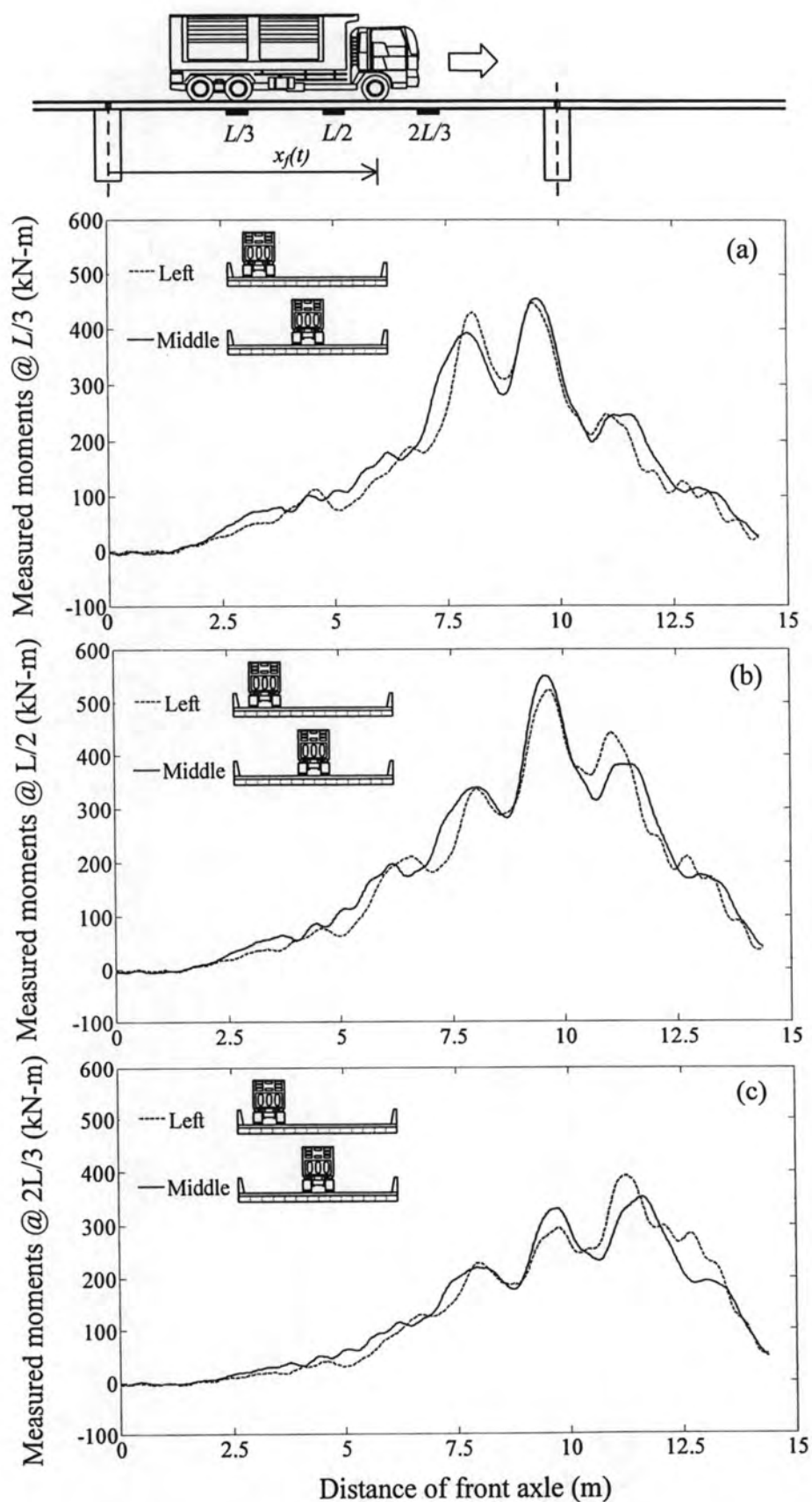
Figure 6.11 Typical measured bending moments (**Z**) of bridge under a passage of truck on left and middle lanes at sections: (a) *L*/3 (b) *L*/2 and (c) 2*L*/3

111

6.6 Axle Weight Estimations

In the following, the effectiveness of the two identification methods through the full-scale tests is investigated. The tests were conducted for various truck weights, speeds and travelling paths. The comparative study is investigated the estimation accuracy on method I and method II. About 47 different conditions of passing trucks are considered. During the passage of the truck, the bending moments of the bridge at three sections, i.e. $L/3$, $L/2$ and $2L/3$ as well as the position of the truck are measured and used as the inputs for axle load identification. The identification utilizes the vehicle-bridge model outlined in previous sections. The model is calibrated by adjusting the section modulus of the bridge so that predicted bridge bending moments at three sections match the corresponding strains obtained from the measurement under a test truck at very slow speed for each lane as described in previous section. Figures 6.12(a) and 6.12(b) compare, respectively, the front and rear dynamic axle loads of the truck identified by the Method I and Method II for the case of the 230 kN truck moving at moderate speed in the left traffic lane. It should be noted that the Method I yields directly the front and rear axle weights of the truck. While the method II firstly yields the time-varying magnitudes of axle loads which, consequently, can be averaged to estimate the corresponding axle weights of the truck.

The effect of regularization parameter is very essential and needed to be conducted for Method II (regularization method with USC), In order to overcome the difficulty in regularization parameter selection to obtain the accurate solution for various conditions of vehicle passages, the range of appropriate regularization parameter assigned in the USC algorithm is determined. Figure 6.13 shows the estimation error with different order of regularization parameter for the case of the 230 kN truck moving at moderate speed in the left traffic lane. The acceptable range for parameter selection can be observed. The regularization parameter for the Method II is found to be not sensitive and can be fixed to any number from 1 to 20. However, for convenience, the value of 10.0 is simply adopted in this full-scale test investigation.
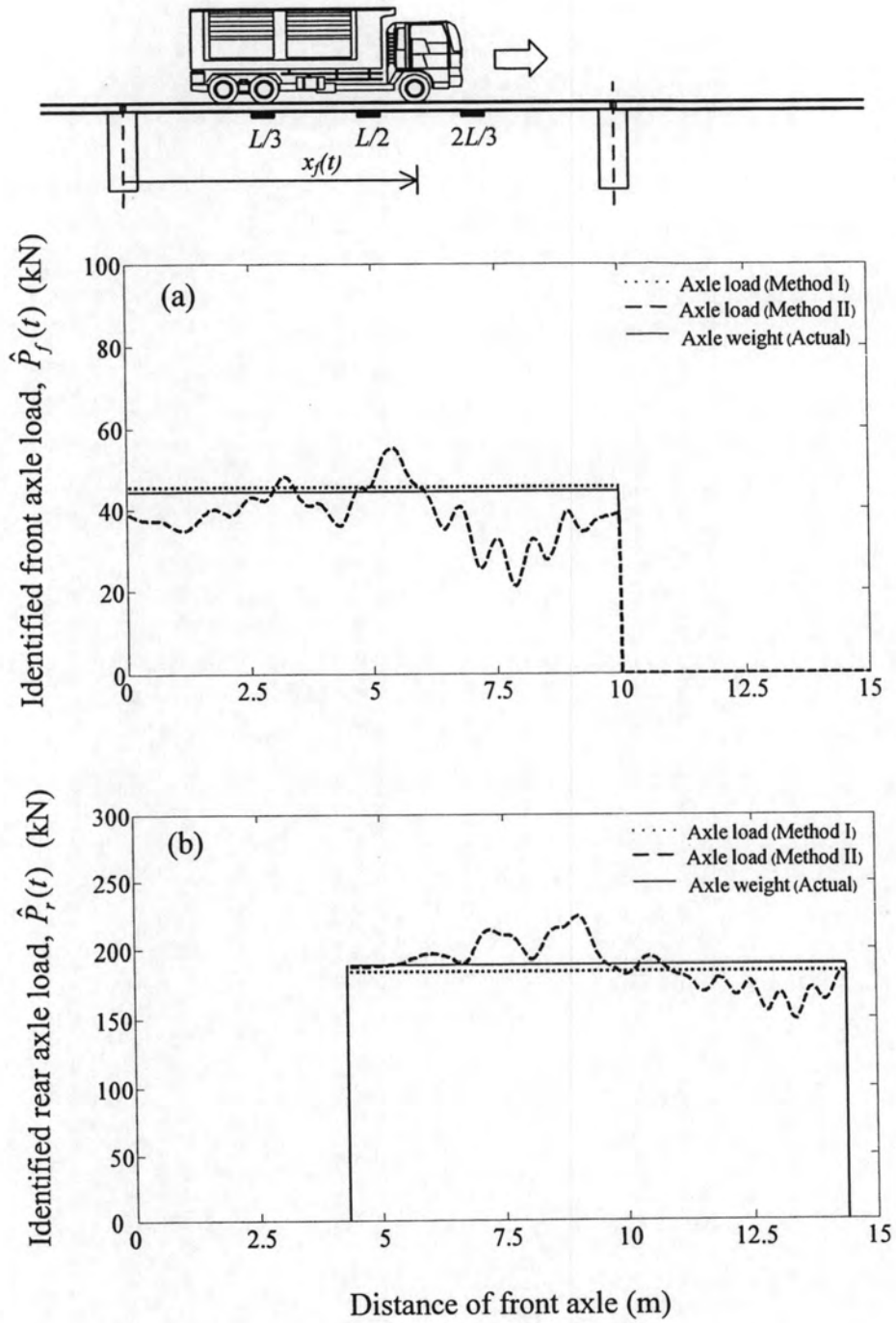
Figure 6.12 Identification results of the axle loads of truck for (a) front axle load and (b) rear axle load
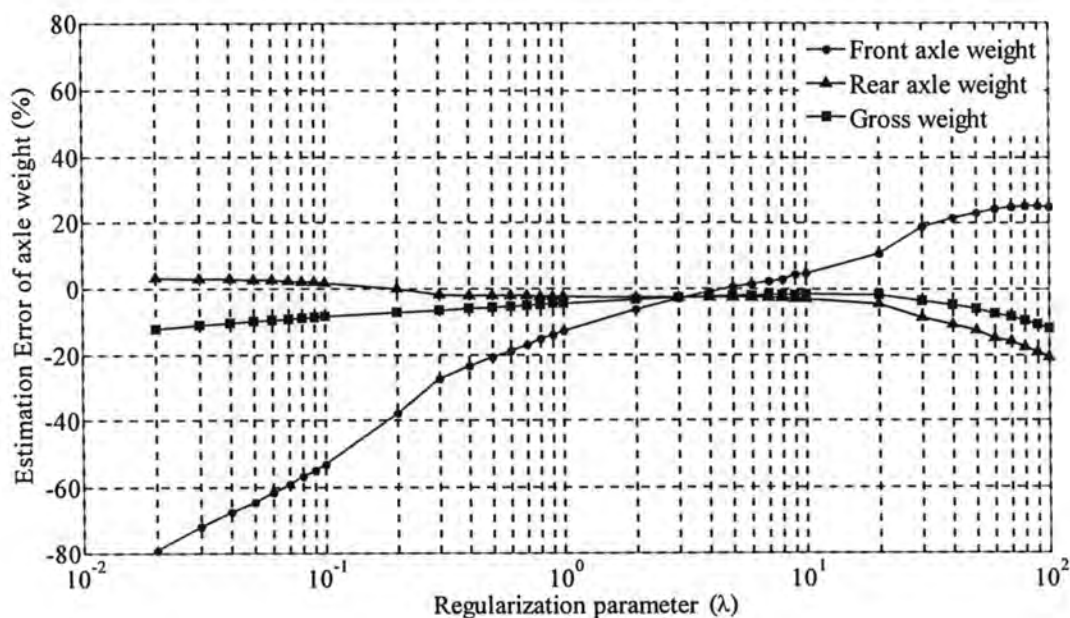
Figure 6.13 Plot of estimation error of axle weight from various order of regularization parameter

6.6.1 Effect of Vehicle Weight and Moving Speed

Figures 6.14(a) and 6.14(b) present the average estimation errors of the obtained axle weights of trucks with various weights and moving speeds identified from Method I and Method II, respectively. From the full-scale test results, similar to the small-scale test results, the axle weight estimation errors are not clearly affected by the vehicle weights and moving speeds. This is because the both identified algorithms, i.e. Method I and Method II, involve the averaging process in determination of axle weights. Therefore their estimated ˙axle weights are not significantly influenced by the fluctuation of dynamic load induced by high speed truck. Although the experimental investigation has shown that the vehicle speed can strongly affect the estimated axle weights, it is shown from this full-scale investigation that the truck speeds are not significantly affected the estimated axle weights, if the range of speeds is about 18–45 km/hr which are compared ·with 5 m/sec to 12 m/sec in the numerical simulation. These speed ranges are not higher than speed ranges in numerical simulation which affect the accuracy of axle weight estimation (vehicle speed >20m/sec). This is because the vehicle speeds in the experimental test did not significantly affect the accuracy of axle weight estimation methods.

6.6.2 Effect of Travelling Paths of Vehicle

The effect of travelling paths of vehicle is also investigated in the full-scale tests. Due to the difficulty on conducting the test in the right traffic lane, only the travelling paths in the left and middle traffic lanes are investigated. Figures 6.15(a) and 6.15(b) presents the average estimation errors of the obtained axle weights under various truck weight and travelling paths identified from Method I and Method II, respectively. The results indicate that the axle weight estimation errors are not strongly affected by truck travelling paths. In particular, it is observed that the estimation errors on truck gross weight of all case are below 6% for both methods. Therefore, using the average sectional bending moment converted from strain gauges distributed in each section as the input responses is sufficient and effective.

6.6.3 Effectiveness of Estimation Methods

Based on these 47 runs of tests, Table 6.3 lists the estimation errors of axle weight from Method I and Method II. The statistical values of the obtained results are listed in Table 6.4. Obviously from the table, the two methods provide quite accurate weight estimations of the vehicle, i.e. errors of gross weight $< \pm 6\%$, in almost of the all cases. From the obtained estimation results, the axle weight estimation errors are not clearly affected by the truck weights, speeds and transverse travelling paths. It is observed that the errors of the front axle weights are usually higher than the associated rear axle and gross weights. This is mainly because the estimation error is computed in term of percentage error with respected to the corresponding actual weight. Therefore, with the same amount of weight error, an axle with lighter weight would give a higher percentage of error. It is also found that the accuracy of estimation method is not affected by using the average sectional bending moment concept. This concept can be used effectively for both axle weight estimation methods. Comparing the errors from both identification methods, it is observed that the Method II is slightly better than Method I. However, the obtained results from both methods can achieve the accuracy level of the WIM system of type-III. These obtained full-scale test results indicate that the proposed B-WIM system can be readily applied to actual bridge to actually monitor truck data in normal traffic condition which will be considered in the next chapter.

The CPU processing time is also investigated to compare the computing speeds of Method I and Method II. Based on 47 full-scale test results, the processing

times required by both methods are listed in Table 6.5. In this study, a personal computer with Intel ® Core ™ 2 Duo 2.4 GHz and 2.0GB RAM is employed and the listed processing times are normalized by 100 data points of input bridge moment histories. The table indicates that the Method I consumes the CPU processing time about 0.6 – 1.5 seconds to complete the axle weights estimation. While, for the Method II, since the method needs about 6-8 rounds to iteratively identify the axle loads. It spends about 4-10 seconds to complete the axle weights estimation. Comparing between both methods, it is clearly found that the Method I can shorten the processing time almost 6 times over the Method II. However, the Method II provides not only the estimated axle weight of the vehicle but also its dynamic axle loads.

6.7 Summary

The effectiveness of the vehicle weight estimations is investigation through full-scale tests. The measured bending moments of the simply-supported bridge at selected sections under a passage of the truck are used as the input for the vehicle weight estimations. Two weight estimation methods assuming constant magnitudes (Method I) and time-varying magnitudes (Method II) of the vehicle axle loads are investigated. Their estimation accuracy are evaluated and compared under various conditions of passing trucks.

Generally, the obtained full-scale test results are similar to those obtained from the small-scale tests. The truck weights, speeds and transverse travelling paths are not clearly affected the accuracy of the both estimation methods. Comparing between the two methods, it is observed that the Method II is slightly better than Method I. Although Method I can shorten the processing time almost 6 times over the Method II, it cannot provide the dynamic axle loads of the passing truck. The selection of the method therefore depends on the required outputs from the B-WIM.

Based on the obtained full-scale test results, the Method I and Method II can achieve the accuracy level of the WIM system of type-III (the gross weight estimation error within ± 6 %). These results indicate that the test system and the estimation methods can be used as a B-WIM in the normal traffic condition with acceptable accuracy.
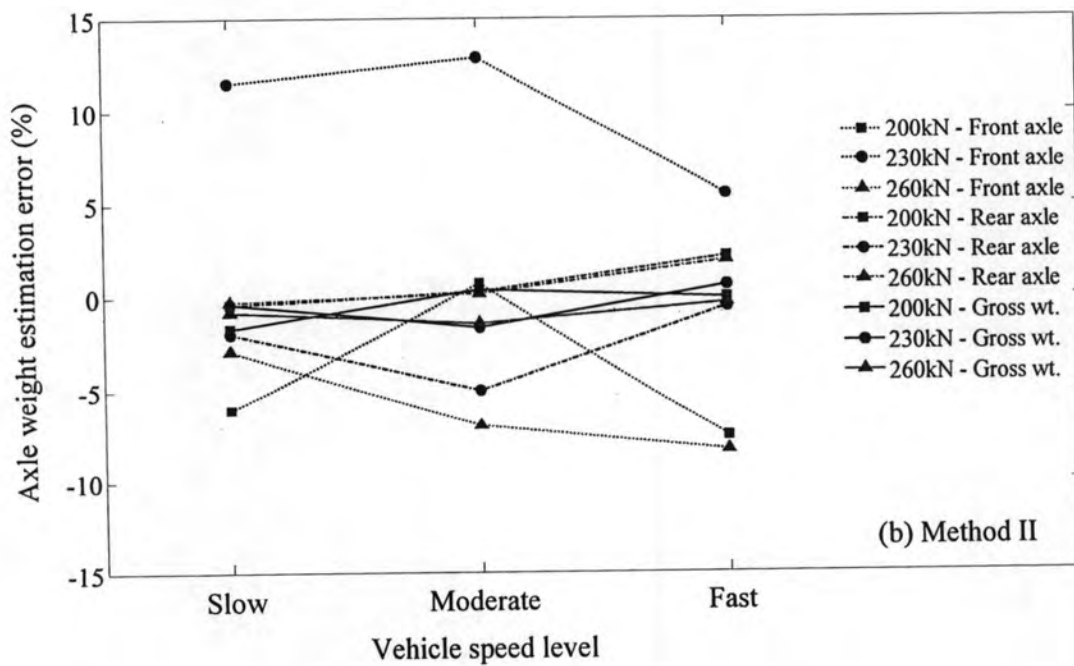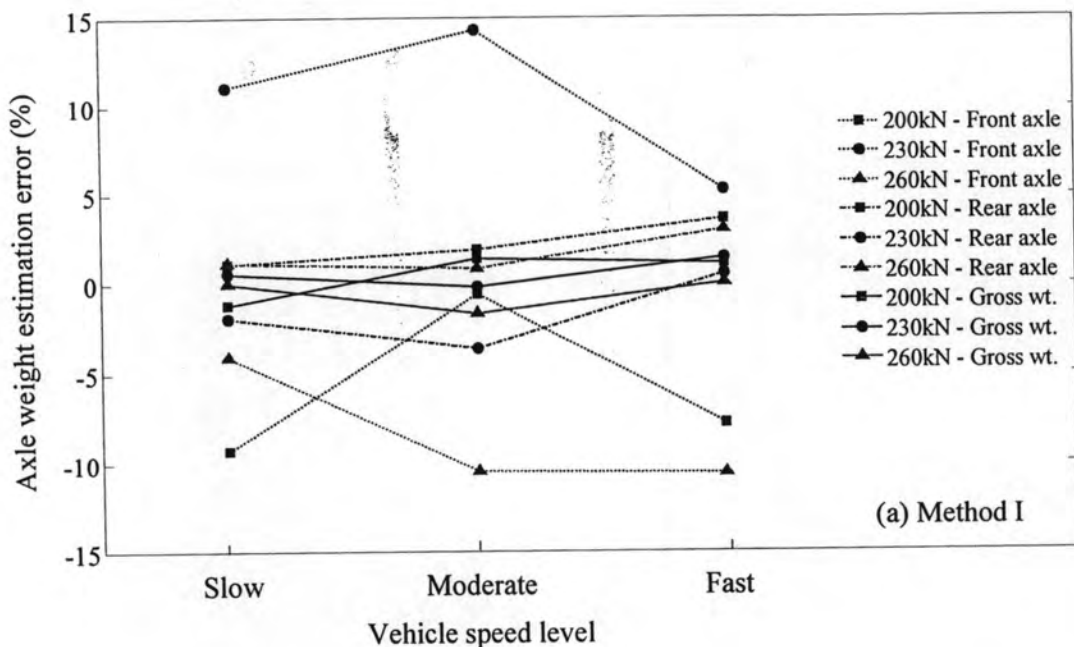
Figure 6.14 Estimation errors of axle weights under various vehicle weights and vehicle speeds using (a) Method I and (b) Method II
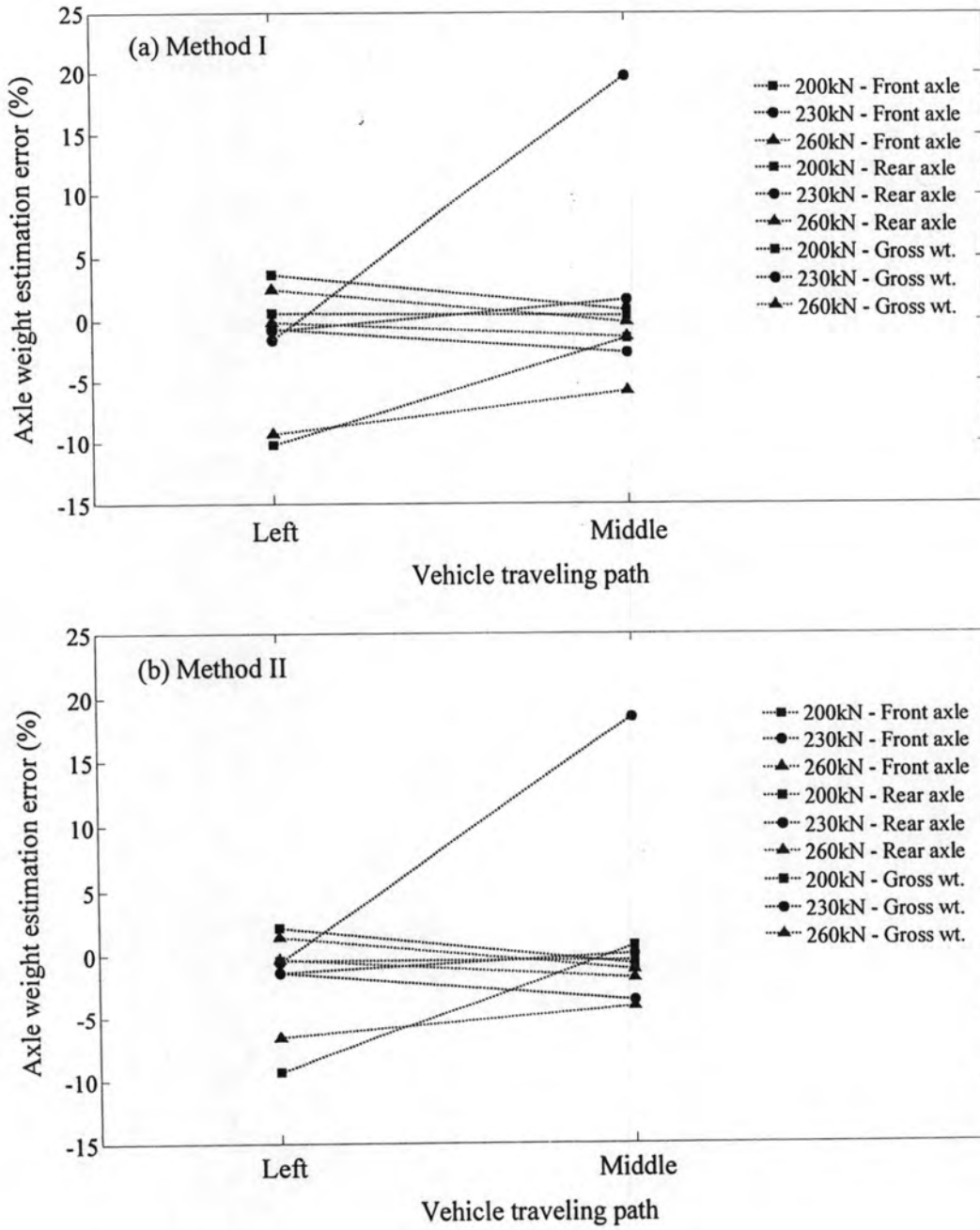
Figure 6.15 Estimation errors of axle weights under various vehicle weights and vehicle travelling paths using (a) Method I and (b) Method II

Table 6.3 Estimation errors of axle weights using the Method I and Method II

Truck weight (kN)	speed	Estimation error (%)	Left Test number			Average	Middle Test number			Average
			1	2	3		1	2	3	
200	Slow	Front axle	-19.3	-9.4	-3.2	**-10.6**	-9.7	-5.8	-8.2	**-7.9**
			(-16.1)	(-8.6)	(-0.7)	**(-8.5)**	(-6.9)	(-4.4)	(-0.2)	**(-3.8)**
		Rear axle	5.7	0.6	0.2	**2.2**	-0.2	0.0	0.2	**0.0**
			(4.3)	(-1.7)	(-2.0)	**(0.2)**	(-1.6)	(-1.6)	(-0.1)	**(-1.1)**
		Gross	0.2	-1.6	-0.5	**-0.6**	-2.3	-1.3	-1.7	**-1.8**
			(-0.2)	(-3.2)	(-1.7)	**(-1.7)**	(-2.7)	(-2.2)	(-0.1)	**(-1.7)**
	Moderate	Front axle	-17.1	-19.1	17.0	**-6.4**	2.8	18.2	-5.1	**5.3**
			(-16.6)	(-18.3)	(15.9)	**(-6.3)**	(6.2)	(20.7)	(-3.7)	**(7.7)**
		Rear axle	4.4	5.7	-1.7	**2.8**	2.6	1.9	-1.2	**1.1**
			(3.2)	(4.3)	(-3.5)	**(1.3)**	(0.9)	(-0.3)	(-3.2)	**(-0.9)**
		Gross	-0.4	0.2	2.4	**0.7**	2.7	5.5	-2.1	**2.0**
			(-1.2)	(-0.7)	(0.8)	**(-0.4)**	(2.0)	(4.4)	(-3.3)	**(1.0)**
	Fast	Front axle	-13.0	-15.0	-13.4	**-13.8**	-2.0	-3.8	0.7	**-1.7**
			(-12.9)	(-14.3)	(-13.1)	**(-13.4)**	(-2.2)	(-4.1)	(0.9)	**(-1.8)**
		Rear axle	5.4	6.6	6.1	**6.0**	-1.2	3.7	1.4	**1.3**
			(4.0)	(5.1)	(4.7)	**(4.6)**	(-3.2)	(2.0)	(-0.1)	**(-0.4)**
		Gross	1.3	1.8	1.8	**1.6**	-1.4	2.0	1.3	**0.6**
			(0.3)	(0.8)	(0.7)	**(0.6)**	(-3.0)	(0.7)	(0.1)	**(-0.7)**
230	Slow	Front axle	1.1	-2.7	-	**-0.8**	19.2	23.8	14.0	**19.0**
			(1.2)	(1.2)	-	**(1.2)**	(18.7)	(25.0)	(11.4)	**(18.4)**
		Rear axle	-1.3	-1.2	-	**-1.3**	-4.0	-2.7	-0.4	**-2.4**
			(-1.5)	(-1.0)	-	**(-1.3)**	(-3.2)	(-2.7)	(-1.3)	**(-2.4)**
		Gross	-0.9	-1.5	-	**-1.2**	0.4	2.3	2.4	**1.7**
			(-1.6)	(-0.8)	-	**(-1.2)**	(-1.1)	(0.9)	(0.5)	**(0.1)**
	Moderate	Front axle	3.6	1.3	-	**2.5**	30.7	12.8	23.1	**22.2**
			(3.1)	(-0.2)	-	**(1.5)**	(26.6)	(12.7)	(22.0)	**(20.4)**
		Rear axle	-1.8	-2.8	-	**-2.3**	-7.6	-3.6	-2.1	**-4.4**
			(-2.8)	(-4.1)	-	**(-3.5)**	(-9.3)	(-5.3)	(-3.7)	**(-6.1)**
		Gross	-0.8	-2.0	-	**-1.4**	-0.3	-0.5	2.7	**0.6**
			(-1.7)	(-3.4)	-	**(-2.6)**	(-2.5)	(-1.9)	(1.2)	**(-1.1)**
	Fast	Front axle	-2.3	-10.8	-	**-6.6**	4.6	-	29.6	**17.1**
			(-0.7)	(-8.4)	-	**(-4.6)**	(3.5)	-	(27.6)	**(15.6)**
		Rear axle	-0.3	3.3	-	**1.5**	2.1	-	-2.8	**-0.4**
			(-1.1)	(2.2)	-	**(0.6)**	(1.0)	-	(-4.3)	**(-1.7)**
		Gross	-0.7	0.6	-	**-0.1**	2.6	-	3.3	**3.0**
			(-1.1)	(0.2)	-	**(-0.5)**	(1.5)	-	(1.7)	**(1.6)**
260	Slow	Front axle	-6.7	-3.8	-2.5	**-4.3**	-2.2	5.3	-14.8	**-3.9**
			(-6.5)	(-2.7)	(-0.4)	**(-3.2)**	(-1.9)	(5.6)	(-11.3)	**(-2.5)**
		Rear axle	1.2	1.1	4.0	**2.1**	-1.1	0.6	1.0	**0.2**
			(-0.1)	(-0.6)	(2.2)	**(0.5)**	(-2.6)	(-0.9)	(0.3)	**(-1.1)**
		Gross	-0.5	0.0	2.6	**0.7**	-1.4	1.6	-2.4	**-0.7**
			(-1.5)	(-1.0)	(1.6)	**(-0.3)**	(-2.5)	(0.5)	(-2.3)	**(-1.4)**
	Moderate	Front axle	-16.6	-11.0	-11.9	**-13.2**	4.0	-16.7	-10.5	**-7.7**
			(-11.2)	(-7.5)	(-6.5)	**(-8.4)**	(4.4)	(-11.8)	(-9.7)	**(-5.7)**
		Rear axle	1.4	1.5	3.5	**2.1**	0.6	-1.0	-0.9	**-0.4**
			(1.2)	(0.9)	(2.7)	**(1.6)**	(-0.7)	(-1.3)	(-2.1)	**(-1.4)**
		Gross	-2.5	-1.3	0.1	**-1.2**	1.4	-4.4	-3.0	**-2.0**
			(-1.5)	(-0.9)	(0.7)	**(-0.6)**	(0.4)	(-3.6)	(-3.8)	**(-2.3)**
	Fast	Front axle	-17.2	-7.0	-7.6	**-10.6**	-	-	-	-
			(-14.6)	(-7.0)	(-3.6)	**(-8.4)**	-	-	-	-
		Rear axle	3.8	2.7	2.5	**3.0**	-	-	-	-
			(2.3)	(1.5)	(1.9)	**(1.9)**	-	-	-	-
		Gross	-0.8	0.6	0.3	**0.0**	-	-	-	-
			(-1.4)	(-0.3)	(0.7)	**(-0.4)**	-	-	-	-

Remark: The numbers in the brackets (.) are the estimation errors from Method II.

Table 6.4 Statistical values of axle weight estimation errors using the Method I and Method II

Method	Weight	Min (%)	Max (%)	Mean (%)	SD
	Front Axle	-19.3	30.7	-1.6	13.1
I	Rear Axle	-7.6	6.6	0.8	3.0
	Gross weight	-4.4	5.5	0.1	2.0
	Front Axle	-18.3	27.6	-0.4	12.0
II	Rear Axle	-9.3	5.1	-0.5	2.9
	Gross weight	-3.8	4.4	-0.7	1.7

Table 6.5 Comparison on CPU processing times from full-scale tests

Method	Method I			Method II		
	Min	Max	Avr.	Min	Max	Avr.
Total processing time (s)	0.6	1.5	1.0	4.9	9.5	6.8